

Article

Black Phosphorus Coated D-Shape Fiber as a Mode-Locker for Picosecond Soliton Pulse Generation

Turki Ali Alghamdi ¹, Somaya Adwan ², Hamzah Arof ² and Sulaiman Wadi Harun ^{2,*}

¹ Department of Computer Sciences, Faculty of Computer and Information Systems, Umm Al-Qura University, Makkah 24382, Saudi Arabia; taghamdi@uqu.edu.sa

² Department of Electrical Engineering, Faculty of Engineering, University of Malaya, Kuala Lumpur 50603, Malaysia; s.adwan@um.edu.my (S.A.); ahamzah@um.edu.my (H.A.)

* Correspondence: swharun@um.edu.my

Abstract: We demonstrate the production of a picosecond pulse from an Erbium laser cavity using black phosphorous (BP) on side-polished fiber saturable absorber (SA) as a mode-locker. The surface of the fiber was removed utilizing a polishing wheel, and then BP was mechanically deposited onto it to develop an excellent evanescent field on the polished surface area. The SA device was used in a 56 m long Erbium-doped fiber laser (EDFL) ring cavity to generate soliton mode-locked pulses with a center wavelength of 1556.2 nm and a 3 dB spectral bandwidth of 2.2 nm. Stable 3.48 MHz soliton pulses with pulse width as short as 1.17 ps were achievable by setting the pump power within 92 mW to 145 mW. The highest pulse energy and peak power obtainable were 5.4 nJ and 4.7 kW, respectively. The results show that BP deposited onto side-polished fiber can be used as an SA in an EDFL cavity. Its easy construction makes it suitable for producing a portable mode-locked laser source.

Keywords: black phosphorus; side-polished fiber; mode-locking; fiber laser



Citation: Alghamdi, T.A.; Adwan, S.; Arof, H.; Harun, S.W. Black Phosphorus Coated D-Shape Fiber as a Mode-Locker for Picosecond Soliton Pulse Generation. *Crystals* **2023**, *13*, 740. <https://doi.org/10.3390/cryst13050740>

Academic Editor: Francesco Simoni

Received: 5 April 2023

Revised: 24 April 2023

Accepted: 25 April 2023

Published: 27 April 2023



Copyright: © 2023 by the authors. Licensee MDPI, Basel, Switzerland. This article is an open access article distributed under the terms and conditions of the Creative Commons Attribution (CC BY) license (<https://creativecommons.org/licenses/by/4.0/>).

1. Introduction

Ultrafast pulse fiber lasers have received great interest in recent years due to their compactness, reliability, and stability [1–3]. They have been applied in various fields, including industrial manufacturing, communication, medicine, and military [4–6]. This is attributed to their unique properties of narrow pulse width, high power, and high precision as compared to the conventional continuous wave or Q-switched lasers. To generate picosecond optical pulses in a fiber laser cavity, various mode-locking techniques can be used. Passively mode-locked fiber lasers are generally preferable due to their characteristics, such as self-starting operation, compact structure, free maintenance, and high stability [6,7]. In a passively generated laser setup, a saturable absorber (SA) is needed in the laser cavity to modulate the loss and lock the phase of the oscillating laser. Currently, most commercial mode-locked fiber lasers employ semiconductor saturable absorber mirrors (SESAMs) as SAs [8]. However, SESAMs are expensive to fabricate and possess a narrow saturable absorption band. Therefore, researchers are still fabricating and testing SAs with new materials that can provide higher performance and lower costs.

SAs made of graphene [9], transition metal dichalcogenide (TMD) [10], and topological material (TI) [11] have been reported to have an ultrafast SA property and achieve good mode-locked effects. These 2D material SAs operate in a broad wavelength band and have bandgaps that are thickness dependent. However, their gradually degrading performance and relatively low optical damage threshold deter them from being widely applied. Other materials, such as gold nanorods [12] and fluorinated antimonene [13], were also reported to have potential for SA application. For instance, Zhang et al. [13] generated Q-switched pulses in Nd:LuAG laser cavity using a fluorinated antimonene-based SA as a Q-switcher. The laser produced a pulse train at the frequency of 733.1 kHz with a pulse duration as short as 326.7 ns.

Another 2D material that catches the interest of researchers is black phosphorus (BP). Although BP can be considered a new entrant to the SA circle, its applications in the fields of electronics and optoelectronic devices are well-known [14–17]. This is due to its noticeable advantages in terms of electron mobility and direct bandgap. The bandgap of this material can be adaptively changed by tuning the number of layers. Moreover, it could be mechanically exfoliated since it is structured from the elemental “phosphorus.” Previously, Q-switched and mode-locked laser generations have been demonstrated where mechanically exfoliated multi-layer BP was utilized as SA [18,19]. The Q-switched pulse laser was produced using an SA constructed of mechanically exfoliated BP crystal and pasting the acquired BP flakes onto a scotch tape. When the SA was added to the ytterbium-doped fiber laser (YDFL) cavity, Q-switched pulses were revealed [18]. Using a different SA made of a few layers of BP, Hisyam et al. demonstrated a mode-locked fiber laser operating at 1085.58 nm with 13.5 MHz repetition frequency and maximum attainable energy of 5.93 nJ [19].

One of the easiest ways to construct an SA is by placing a thin film containing a suitable material between two fiber ferrules. When the SA is placed in a laser cavity, a mode-locked or Q-switched fiber laser is generated. However, this method entails a parasitic loss associated with the thin film and the end face of the fiber ferrules [20]. In this study, we introduce mode-locked fiber laser generation using BP SA. The BP is deposited onto a side-polished fiber utilizing a mechanical exfoliation technique so that the BP can efficiently interact with the oscillating laser via an evanescent field. To our knowledge, this is the first experiment of mode-locked pulse generation using BP deposited onto side-polished fiber in an Erbium-doped fiber laser (EDFL) cavity. Compared to the previous method of placing a thin film between two fiber ferrules, the proposed SA based on putting BP onto the SPF is expected to provide a significantly higher damage threshold. Previously, Liu et al. reported a Q-switched EDFL based on BP thin film with a minimum pulse duration of 7.11 μ s [21]. The proposed EDFL based on SPF provides a significantly smaller pulse duration of 1.17 ps via a mode-locking mechanism.

2. Preparation of a Saturable Absorber Device

In this study, another novel 2D material, BP, is used as an SA material. It is the most thermodynamically stable allotrope of phosphorus with high electron mobility, and thus it has great potential for both electronics and photonics applications. Similar to graphite, BP is a layered material in which adjacent BP atomic layers are stacked together through weak van der Waals interaction. Since the BP only comprises one element component and has the same direct bandgap as graphene, it is expected that it can also be employed as SA for pulse generation. Here, the BP-based SA was fabricated using the cost-effective mechanical exfoliation technique. The few graphene layers were mechanically exfoliated onto an SPF to allow the interaction between the oscillating laser and the phosphorus materials for mode-locking operation.

At first, we fabricated a simple side polisher which consists of a dc motor attached to a cylindrical PVC shaft that turns a small grinder as shown in Figure 1a. The motor is powered by a variable DC voltage supply of 0–17 V with a maximum power of 12 W. This allows the speed of the grinder to be changed manually using a knob. The surface of the grinder is sandpaper of grit size 1000 cw. The operating speed of the grinder is increased slowly and then maintained when the fiber starts to show a grinding trace on its surface. A pair of optical fiber holders are used to hold the fiber straight while its surface is being polished. The fiber chosen as the SA is a commercially available SMF-28 silica fiber with a 125 μ m cladding diameter. One end of the fiber is connected to a 1550 nm light source while the other end is attached to an Optical Power Meter (OPM) so that the power that flows through it can be monitored in real time. Once the polishing process starts, it continues until the insertion loss of the fiber increases from its reference value by approximately 2 dB. The side-polished fiber is then analyzed under a medilux-12 microscope to measure its waist diameter as shown in Figure 2b. For our experiment, the waist diameter was about 92 μ m. Consequently, a BP SA was prepared by transferring BP crystal onto the

side-polished fiber using the mechanical exfoliation method as depicted in Figure 1c. Since the fiber becomes fragile after the side polishing, we placed the SPF onto a glass substrate to protect and improve the robustness of the SA device.

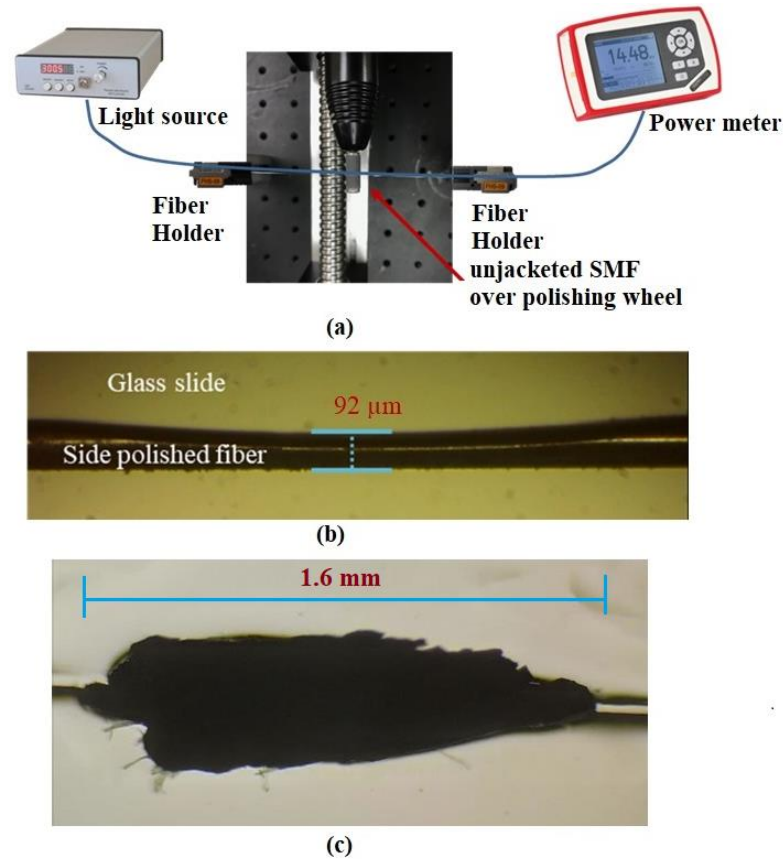


Figure 1. (a) Fabrication setup for side-polished fiber; (b) microscopic image of the prepared side of the polished fiber; (c) image of BP coated over side-polished fiber.

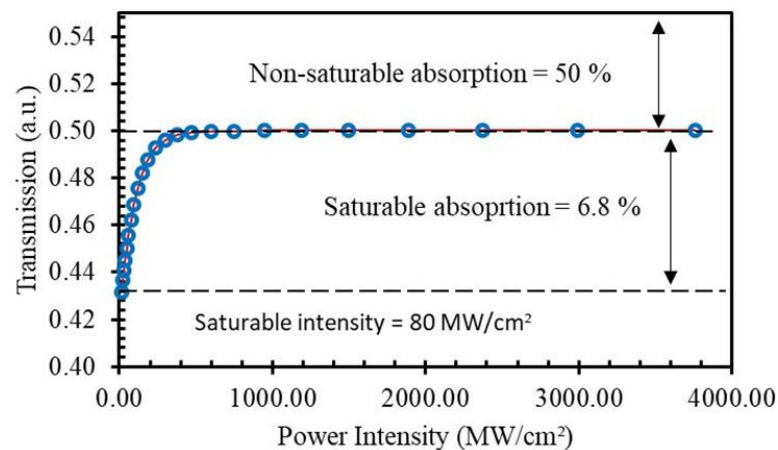


Figure 2. Nonlinear transmission profile conforming to the capability of the BP-based SA to convert CW light into repetitive ultra-short pulses. The blue dots represent the experimental data while the red curve is the fitting line.

The nonlinear characteristics of the BP-based SA were determined using a two-arms detector method. We employed a home-built mode-locked fiber laser operating at 1557.7 nm as the light source. The repetition frequency and pulse duration of the laser source were 1.88 MHz and 3.46 ps, respectively. The mode-locked laser pulses were then amplified using

a homebuilt optical amplifier (Erbium-doped fiber amplifier). An external variable optical attenuator was used after the amplifier to control the output intensity of the amplified laser. It was then split equally into two paths by a 3 dB coupler. One path was launched into the SA under test while another path was used as a reference. The measured nonlinear transmission curve is shown in Figure 2, which indicates the sharp increase in the light transmission before it is gradually saturated with a further increase of pulse fluence or peak laser intensity. The phenomenon proves that the BP SA sample possesses a good saturable absorption property. The SA parameters can be obtained by fitting the data utilizing the following formula:

$$T(I) = 1 - \Delta T \times \exp(-I/I_{sat}) - T_{ns}$$

where $T(I)$ is the transmission, I is the incident peak intensity, ΔT is the saturable absorption or modulation depth, I_{sat} is the saturation peak intensity, and T_{ns} is the non-saturation loss. As seen in the figure, the BP deposited onto side-polished fiber records a saturable absorption (modulation depth) of 6.8%, non-saturable loss of 50%, and saturation intensity of 80 MW/cm², thus confirming the SA capability to convert CW light into repetitive ultra-short pulses in a fiber laser cavity. The non-saturable loss is relatively large due to the use of SPF, which exhibits a high insertion loss.

3. Experimental Details

The schematic of the laser's configuration based on BP-coated polished fiber SA is depicted in Figure 3. The BP-coated polished fiber is introduced into the resonator as a mode-locker. The cavity consists of a 2.4 m long Erbium-doped fiber (EDF, Fibercore I-25), which is pumped using a 980 nm diode laser (LD) via a wavelength-division multiplexer (WDM) to provide population inversion for lasing. The EDF has an Erbium ion absorption of 23 dB/m at 980 nm while its core diameter and numerical aperture are 4 μm and 0.16, respectively. Other supporting devices, including an isolator, an additional single mode-fiber (SMF) spool, and an optical coupler are necessary so that the total cavity length becomes about 56 m. The additional SMF helps manage the nonlinearity and dispersion of the cavity. The group velocity dispersion at the 1550 nm region for SMF and EDF used in this oscillator are -21.7 and 27.6 ps²/km, respectively. Thus, the total cavity dispersion is about -1.1 ps², which assists the formation of soliton. The optical isolator placed between EDF and SA ensures a unidirectional propagation of light in the cavity. The 20/80 coupler is used to tap out 20% of light for analysis while trapping the remaining 80% of the intensity inside the cavity for oscillation. The output pulses are examined via a series of measurement devices including an optical spectrum analyzer (ANRITSU: MS9710C, 0.07 nm spectral resolution), a 350 MHz digital oscilloscope (GWINSTEK: GDS-3352), a commercial autocorrelator (AInair HAC200), and an RF spectrum analyzer (ANRITSU: MS2683A). A 1.2 GHz InGaAs fast photodetector (THORLABS: DET01CFC) is used to convert the optical signal to an electrical signal. A polarization controller (PC) was excluded from the setup since we observed that polarization plays an insignificant role in the mode-locking operation of the laser. From trial and error, we obtained a similar outcome with the presence of a PC in the resonator. It is worth noting that the lengths of the active and passive intracavity fibers were optimized for the mode-locking operation.

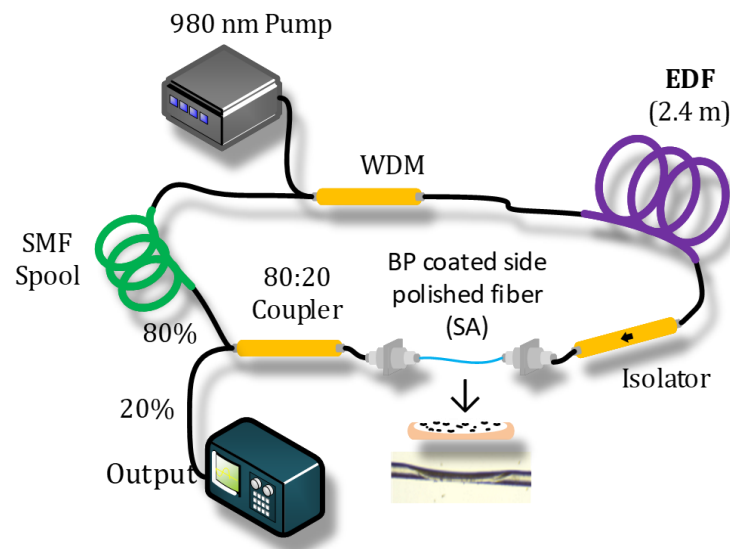


Figure 3. The EDFL configuration with the exfoliated BP on SPF as a mode-locker. A 50 m long SMF spool was added to optimize the cavity nonlinearity and dispersion for assisting in the mode-locking operation.

4. Discussion

As the 980 nm pump is launched into the EDF, it produces photons via the spontaneous emission process, which are then amplified to generate amplified spontaneous emission (ASE) due to the stimulated emission process. The ASE oscillates in the ring EDFL to generate many laser modes. Each of these modes oscillates independently, with no fixed relationship between each other. The individual phase of the light waves in each mode is not fixed and may vary randomly due to many factors including thermal changes in the gain medium. By incorporating an SA device into the EDFL cavity, each mode operates with a fixed phase between it and the other modes instead of oscillating independently. This is attributed to the SA, which behaves differently depending on the intensity of the light passing through it. It exhibits an intensity-dependent transmission by selectively absorbing low-intensity light but transmitting light of sufficiently high intensity. As the light in the cavity oscillates, the modes of the laser will periodically all constructively interfere with one another, producing a train of pulses and mode-locking of the laser. These pulses occur separated in time by $\tau = 2L/c$, where τ is the time taken for the light to make exactly one round trip of the laser cavity. This time corresponds to a frequency exactly equal to the mode spacing of the laser, $\Delta\nu = 1/\tau$.

In the beginning, the EDFL cavity was tested without the BP SA to check whether the self-starting mode-locked laser operation existed in the laser cavity. However, only continuous-wave operation could be spotted on the oscilloscope despite varying the pump power. Then, the prepared BP-based SA was added to the cavity and a stable mode-locked laser operation was observed as the pump power was increased and stayed in the range of 92 mW to 145 mW. This suggests that no other optical mechanisms, including non-linear polarization evolution, could lead to mode-locking.

A summary of the characteristics of the mode-locked pulses is presented in Figure 4. Figure 4a shows the sketch of the pulse train within a time span of 12 μ s as observed by an oscilloscope at the pump power of 145 mW. The enlarged pulse train with triple pulses is shown in Figure 4b. At this pump power, the pulse period is 287.2 ns, which corresponds to an oscillation of 3.48 MHz. This figure matches very well with the cavity length of around 56 m. The pulse width of the mode-locked pulse is measured using an autocorrelator and compared with the sech² fitting curve as shown in Figure 4c. The pulse width is 1.17 ps. It is much shorter than the one reported in an earlier work where an SA based on zinc oxide was used, which was at 400 ns [22].

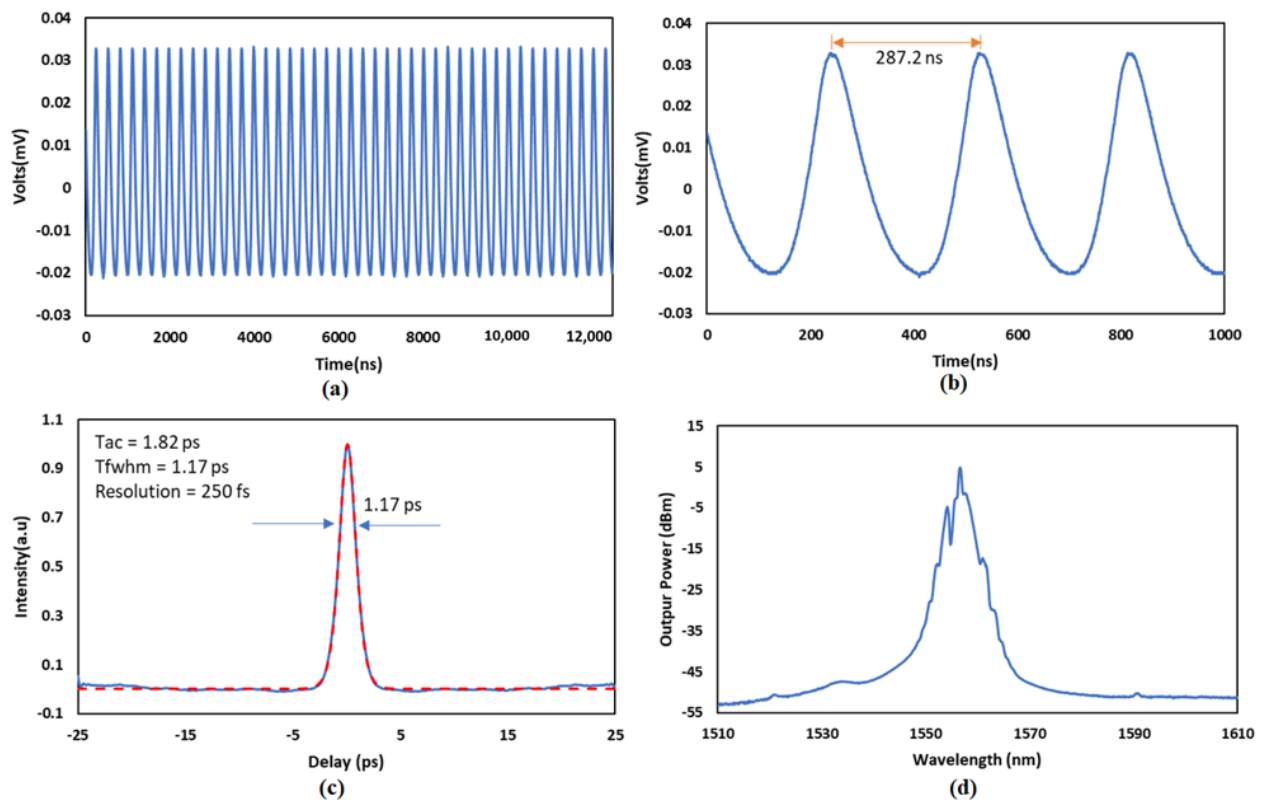


Figure 4. Temporal and spectral characteristics of the mode-locked laser under a pump power of 145 mW. (a) Time domain pulse train; (b) enlarged oscilloscope trace; (c) autocorrelator trace; (d) optical spectrum.

Figure 4d shows the emission spectrum of the mode-locked laser, where Kelly sidebands are clearly seen. This reveals that the mode-locked laser produced soliton pulses, which operate at a center wavelength of 1556.2 nm with a 3 dB bandwidth of about 2.2 nm. The spectral broadening is noticeable due to the self-phase modulation effect while the soliton generation is dominantly induced by the saturable absorption of the BP inside the laser cavity. Based on the spectral bandwidth of output pulses, time–bandwidth product (TBP) is determined to be around 1.0, which reveals that the pulses are chirped.

The relationship between the average output power, pulse energy, and pump power is depicted in Figure 5a. Both output power and pulse energy increase with the increment of pump power. This is attributed to the population inversion, which increases with the pump power. Under a pump power of 145 mW, the highest output power and pulse energy are 19 mW and 5.4 nJ. The peak power of the mode-locked pulse is calculated and plotted against the pump power as illustrated in Figure 5b. Under the pump power of 145 mW, the maximum peak power is 4.7 kW. As the pump power is further increased above 145 mW, the mode-locked pulses become unstable and diminished.

RF spectrum is used to investigate the stability of mode-locked operation under various pump power. Figure 6 shows the RF spectrum recorded within 100 MHz bandwidth under the resolution of 1 kHz when the pump power is fixed at 145 mW. Obviously, many harmonics are obtained within the frequency bandwidth. RF spectrum within a 5.6 MHz bandwidth is also recorded and depicted in the inset of Figure 6. It indicates that the peak of the fundamental frequency is located at 3.48 MHz with a signal-to-noise ratio of more than 70 dB.

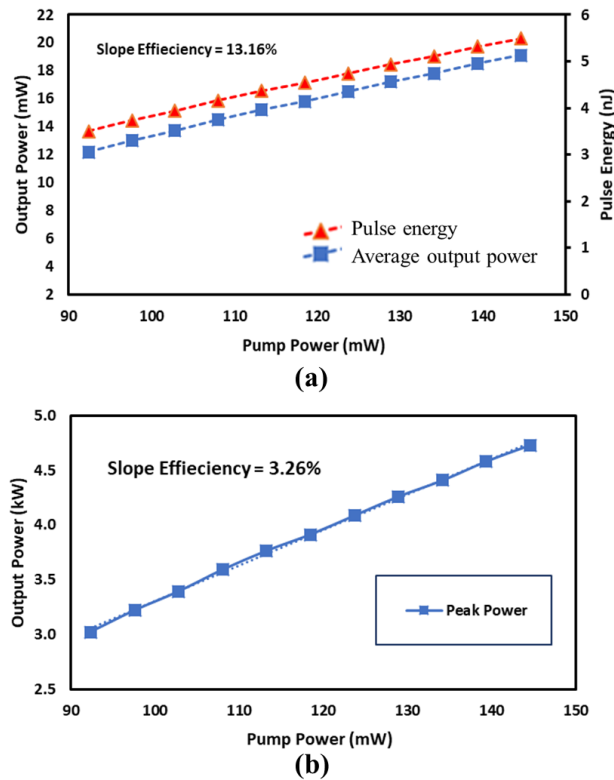


Figure 5. Variation of mode-locked laser parameters with pumping power. (a) Average output power and pulse energy; (b) peak power.

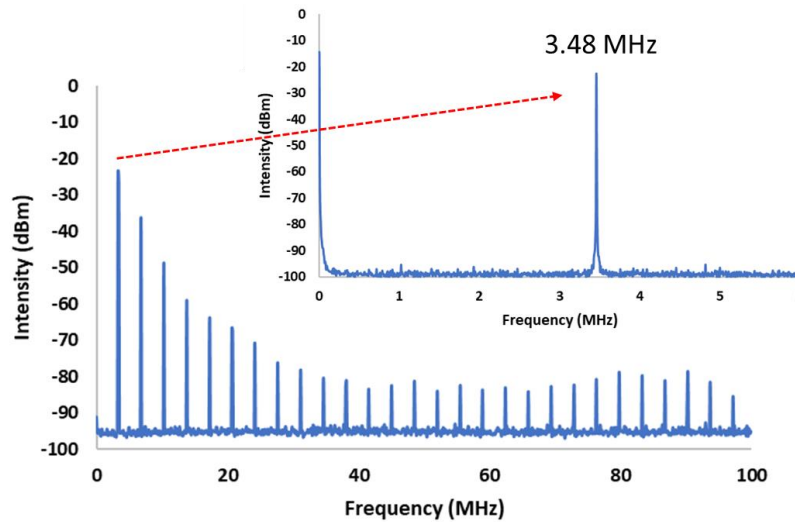


Figure 6. RF spectrum. Inset shows the enlarged spectrum showing the fundamental frequency (red-dashed line).

The proposed ultrashort pulse fiber lasers have numerous potential applications in a wide range of fields, including material processing, medical imaging, microfabrication, optical communication, and spectroscopy [5,6]. However, the energy of our mode-locked laser pulse is only 9.4 nJ. For applications such as precision cutting and drilling, a much higher energy of pulses is required, and the ultrashort laser pulse cannot be directly amplified in optical amplifiers because of damage issues in optical elements due to the nonlinear effect and the low-energy extraction efficiency. These hurdles could be solved by employing the chirped-pulse amplification (CPA) technique, whereby the laser pulses were temporarily stretched before amplification. The energy of the stretched pulse is amplified,

and the pulse width is compressed back to the original level after the amplification. The CPA technique is widely demonstrated in many literatures, and it is also used to produce relativistic laser intensity ($>10^{18}$ W/cm²) [23,24]. Ultrafast manipulation also received great attention in recent years in which structured ultrashort pulses with coupled spatiotemporal properties are used as a key tool [25]. The ultrafast vector beams are useful for applications such as time-resolved imaging, microscopy, particle acceleration, and nonlinear optics.

5. Conclusions

A newly developed, BP-based SA was successfully deployed as a mode-locker in an EDFL cavity to produce a soliton picosecond pulse. To prepare the SA device, the exploited BP was coated onto a side-polished fiber, which was prepared using a polishing wheel technique. The SA has a modulation depth of 6.8% and it functions to establish excellent evanescent field interaction between the BP material and oscillating laser on the surface of the side-polished fiber. Soliton mode-locked laser was achieved in a 56 m long EDFL's ring cavity. It operates stably at 1556.2 nm with a 3 dB spectral bandwidth of 2.2 nm, repetition frequency of 3.48 MHz, and pulse width of 1.17 ps within a pump power range from 92 mW to 145 mW. The maximum pulse energy and peak power were obtained at 5.4 nJ and 4.7 kW, respectively. These results indicate that BP deposited onto side-polished fiber can be deployed as SA in the EDFL cavity for a portable mode-locked laser source. These results reveal that a BP deposited onto side-polished fiber can be used to generate soliton mode-locked pulses, and thus it has a great potential for use in other photonics applications.

Author Contributions: Conceptualization, T.A.A. and S.W.H.; methodology, S.A. and H.A.; formal analysis, T.A.A. and S.W.H.; investigation, T.A.A.; writing—original draft preparation, S.W.H.; writing—review and editing, H.A.; visualization, S.A.; supervision, T.A.A.; project administration, S.A.; funding acquisition, T.A.A. All authors have read and agreed to the published version of the manuscript.

Funding: National Science, Technology and Innovation Plan (MAARIFAH), King Abdulaziz City for Science and Technology (KACST), Kingdom of Saudi Arabia (Grant no.: 14-ELE1454-10).

Data Availability Statement: The data presented in this study are available on request from the corresponding author.

Acknowledgments: The financial support from the National Science, Technology and Innovation Plan (MAARIFAH), King Abdulaziz City for Science and Technology (KACST), Kingdom of Saudi Arabia (Grant no.: 14-ELE1454-10), is acknowledged.

Conflicts of Interest: The authors declare no conflict of interest.

References

1. Wang, P.; Zhang, H.; Yin, Y.; Ouyang, Q.; Chen, Y.; Lewis, E.; Farrell, G.; Tokurakawa, M.; Harun, S.W.; Wang, C.; et al. NiS₂ as a broadband saturable absorber for ultrafast pulse lasers. *Opt. Laser Technol.* **2020**, *132*, 106492. [[CrossRef](#)]
2. Martinez, A.; Sun, Z. Nanotube and graphene saturable absorbers for fibre lasers. *Nat. Photonics* **2013**, *7*, 842–845. [[CrossRef](#)]
3. Wang, H.; Pan, J.; Meng, Y.; Liu, Q.; Shen, Y. Advances of Yb: CALGO laser crystals. *Crystals* **2021**, *11*, 1131. [[CrossRef](#)]
4. Gafner, M.; Kramer, T.; Remund, S.M.; Holtz, R.; Neuenschwander, B. Ultrafast pulsed laser high precision micromachining of rotational symmetric parts. *J. Laser Appl.* **2021**, *33*, 012053. [[CrossRef](#)]
5. Shi, W.; Fang, Q.; Zhu, X.; Norwood, R.A.; Peyghambarian, N. Fiber lasers and their applications. *Appl. Opt.* **2014**, *53*, 6554–6568. [[CrossRef](#)]
6. Fu, W.; Wright, L.G.; Sidorenko, P.; Backus, S.; Wise, F.W. Several new directions for ultrafast fiber lasers. *Opt. Express* **2018**, *26*, 9432–9463. [[CrossRef](#)]
7. Tuo, M.; Xu, C.; Mu, H.; Bao, X.; Wang, Y.; Xiao, S.; Ma, W.; Li, L.; Tang, D.; Zhang, H.; et al. Ultrathin 2D transition metal carbides for ultrafast pulsed fiber lasers. *ACS Photonics* **2018**, *5*, 1808–1816. [[CrossRef](#)]
8. Okhotnikov, O.; Grudinin, A.; Pessa, M. Ultra-fast fibre laser systems based on SESAM technology: New horizons and applications. *New J. Phys.* **2004**, *6*, 177. [[CrossRef](#)]
9. Fu, B.; Hua, Y.; Xiao, X.; Zhu, H.; Sun, Z.; Yang, C. Broadband graphene saturable absorber for pulsed fiber lasers at 1, 1.5, and 2 μ m. *IEEE J. Sel. Top. Quantum Electron.* **2014**, *20*, 411–415.
10. Liu, W.; Pang, L.; Han, H.; Bi, K.; Lei, M.; Wei, Z. Tungsten disulphide for ultrashort pulse generation in all-fiber lasers. *Nanoscale* **2017**, *9*, 5806–5811. [[CrossRef](#)]

11. Mondal, S.; Ganguly, R.; Mondal, K. Topological Insulators: An In-Depth Review of Their Use in Modelocked Fiber Lasers. *Ann. Der Phys.* **2021**, *533*, 2000564. [[CrossRef](#)]
12. Zhang, G.; Liu, T.; Shen, Y.; Zhao, C.; Huang, B.; Kang, Z.; Qin, G.; Liu, Q.; Fu, X. 516 mW, nanosecond Nd: LuAG laser Q-switched by gold nanorods. *Chin. Opt. Lett.* **2018**, *16*, 020011. [[CrossRef](#)]
13. Zhang, G.; Tang, X.; Fu, X.; Chen, W.; Shabbir, B.; Zhang, H.; Liu, Q.; Gong, M. 2D group-VA fluorinated antimonene: Synthesis and saturable absorption. *Nanoscale* **2019**, *11*, 1762–1769. [[CrossRef](#)] [[PubMed](#)]
14. Abbas, A.N.; Liu, B.; Chen, L.; Ma, Y.; Cong, S.; Aroonyadet, N.; Kopf, M.; Nilges, T.; Zhou, C. Black phosphorus gas sensors. *ACS Nano* **2015**, *9*, 5618–5624. [[CrossRef](#)] [[PubMed](#)]
15. Li, L.; Yu, Y.; Ye, G.J.; Ge, Q.; Ou, X.; Wu, H.; Feng, D.; Chen, X.H.; Zhang, Y. Black phosphorus field-effect transistors. *Nat. Nanotechnol.* **2014**, *9*, 372–377. [[CrossRef](#)]
16. Dai, J.; Zeng, X.C. Bilayer phosphorene: Effect of stacking order on bandgap and its potential applications in thin-film solar cells. *J. Phys. Chem. Lett.* **2014**, *5*, 1289–1293. [[CrossRef](#)]
17. Pang, J.; Bachmatiuk, A.; Yin, Y.; Trzebicka, B.; Zhao, L.; Fu, L.; Mendes, R.G.; Gemming, T.; Liu, Z.; Rummeli, M.H. Applications of phosphorene and black phosphorus in energy conversion and storage devices. *Adv. Energy Mater.* **2018**, *8*, 1702093. [[CrossRef](#)]
18. Al-Masoodi, A.H.H.; Ahmed, M.H.M.; Latiff, A.A.; Arof, H.; Harun, S.W. Q-switched ytterbium-doped fiber laser using black phosphorus as saturable absorber. *Chin. Phys. Lett.* **2016**, *33*, 054206. [[CrossRef](#)]
19. Hisyam, M.B.; Rusdi, M.F.M.; Latiff, A.A.; Harun, S.W. Generation of mode-locked ytterbium doped fiber ring laser using few-layer black phosphorus as a saturable absorber. *IEEE J. Sel. Top. Quantum Electron.* **2016**, *23*, 39–43. [[CrossRef](#)]
20. Nizamani, B.; Jafry, A.A.A.; Khudus, M.A.; Memon, F.A.; Shuhaimi, A.; Kasim, N.; Hanafi, E.; Yasin, M.; Harun, S.W. Indium tin oxide coated D-shape fiber as saturable absorber for passively Q-switched erbium-doped fiber laser. *Opt. Laser Technol.* **2020**, *124*, 105998. [[CrossRef](#)]
21. Liu, H.; Song, W.; Yu, Y.; Jiang, Q.; Pang, F.; Wang, T. Black phosphorus-film with drop-casting method for high-energy pulse generation from Q-switched Er-doped fiber laser. *Photonic Sens.* **2019**, *9*, 239–245. [[CrossRef](#)]
22. Alani, I.A.M.; Ahmad, B.A.; Ahmed, M.H.M.; Latiff, A.A.; Al-Masoodi, A.H.H.; Lokman, M.Q.; Harun, S.W. Nanosecond mode-locked erbium doped fiber laser based on zinc oxide thin film saturable absorber. *Indian J. Phys.* **2019**, *93*, 93–99. [[CrossRef](#)]
23. Shen, Y.; Gao, G.; Meng, Y.; Fu, X.; Gong, M. Gain-phase modulation in chirped-pulse amplification. *Phys. Rev. A* **2017**, *96*, 043851. [[CrossRef](#)]
24. Gao, G.; Shen, Y.; Deng, D.; Meng, Y.; He, L.; Gong, M.; Zhang, H. Chirp-coefficient bisection iteration method for phase-intensity reconstruction of chirped pulses. *Opt. Rev.* **2018**, *25*, 598–607. [[CrossRef](#)]
25. Alonso, B.; Lopez-Quintas, I.; Holgado, W.; Drevinskas, R.; Kazansky, P.G.; Hernández-García, C.; Sola, Í.J. Complete spatiotemporal and polarization characterization of ultrafast vector beams. *Commun. Phys.* **2020**, *3*, 151. [[CrossRef](#)]

Disclaimer/Publisher's Note: The statements, opinions and data contained in all publications are solely those of the individual author(s) and contributor(s) and not of MDPI and/or the editor(s). MDPI and/or the editor(s) disclaim responsibility for any injury to people or property resulting from any ideas, methods, instructions or products referred to in the content.